Contents

1 Extensive air showers

Consider a high energy cosmic ray impinging on earth. The questions pertaining to where it might originate from and how it has gained so much kinetic energy have been answered in the preceding **??**. In the following, the particle cascades resulting from the particle interacting in the upper atmosphere will be examined. This is done in a two-fold way. The underlaying principles will be explained via considering a particle carrying no SU(3)-color charge in **??**. The more general treatment for hadronic showers is then found in **??**. As supplementary information, the effect of different hadronic primaries is discussed in **??**.

1.1 Electromagnetic showers

The dominating interaction of $E > 10\,\mathrm{MeV}$ photons in matter is e^+e^- pair production, whereas for electrons/positrons the creation of a γ via bremsstrahlung prevails at high energies. This is shown in **??**. Consequently, an entire cascade of electrons, positrons and photons can emerge from a single primary particle, as realised by Heitler in [**heitler1984quantum**].

Of particular interest in these showers are, apart from the primary particles energy E_0 and arrival direction (Φ, θ), the atmospheric depth X_{max} at which it reaches its' maximum multiplicity, as well as the **L**ateral **D**istribution **F**unction (LDF), that parametrizes the distribution of particles along the shower axis. An important variable that influences both values is the radiation length X_0. It represents the characteristic length at which an $e^{\pm}$ loses $1 - \frac{1}{e} \approx 63\%$ of its energy. It also corresponds to the mean free path of a photon in matter up to a factor $7/9$ [**gupta2010calculation**]. Neglecting said factor and assuming that new particles on average inherit half of the original energy, describing the multitude of particles contained in an electromagnetic shower becomes a counting exercise in the context of the Heitler-model.

With each radiation length, the number of particles N in the shower double, while the energy per particle E_{pp} halves. After traversing an atmospheric depth of $n \cdot X_{\mathrm{max}}$, typically measured in $\frac{\mathrm{g}}{\mathrm{cm}^2}$, they consequently read

$$N(n) = 2^n, \qquad E(n) = \frac{E_0}{2^n}. \tag{1.1}$$

After some time, the energy of each individual particle E_{PP} will have diminished by so much that other processes will dominate over bremsstrahlung and pair production. This occurs at the critical energy E_c below which the shower rapidly stops creating new
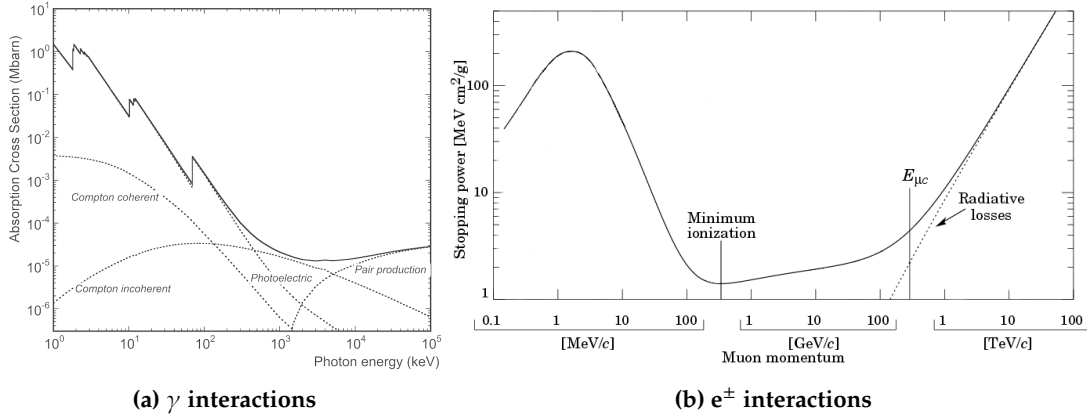
Figure 1.1: (a) Cross section for different energy loss processes of a photon in tungsten. The sudden spikes correspond to the transition energy of increasingly higher-energy electron shells. From [**chen2007interactions**]. **(b)** Stopping power of copper, representatively on an antimuon μ^+, with respect to its' momentum. Plot adopted with changes from [**meroli2017straggling**].

particles and dies out as a result. It follows via **??** and **??** that both $X_{\max}$ as well as $N_{\max}$ increase with E_0. The multiplicity arising from these assumptions alongside a stylized propagation of the thus created shower is represented in **??**.

$$E_{\mathrm{PP}}\left(n_{\max}\right) \overset{!}{=} E_c \overset{(??)}{=} \frac{E_0}{2^{n_{\max}}}$$

$$\Leftrightarrow \qquad n_{\max} = \left\lfloor \log_2\left(\frac{E_0}{E_c}\right) \right\rfloor$$

$$\Rightarrow \qquad X_{\max} = n_{\max} \cdot X_0 = \left\lfloor \log_2\left(\frac{E_0}{E_c}\right) \right\rfloor. \tag{1.2}$$

$$\Rightarrow \qquad N_{\max} = 2^{n_{\max}} = \left\lfloor \frac{E_0}{E_c} \right\rfloor. \tag{1.3}$$

The number of particles at a given distance from the shower axis (y-axis in **??**) is essentially random, but follows a statistical basis, the lateral distribution function. The LDF can either be derived approximately from first principles [**kamata1958lateral**] or empirically, as is done in [**greisen1960cosmic**]. The latter arrives at a closed form approximation for the local density ρ of particles given a shower with multiplicity N at a distance r from the shower axis as

$$\rho_{\mathrm{EM}}(N, r) = \frac{0.4\,N}{r_{\mathrm{M}}^2} \left(\frac{r_{\mathrm{M}}}{r}\right)^{0.75} \left(\frac{r_{\mathrm{M}}}{r + r_{\mathrm{M}}}\right)^{3.25} \left(1 + \frac{r}{11.4\,r_{\mathrm{M}}}\right). \tag{1.4}$$

In **??**, the Molière radius r_{M} characterizes the lateral spread in multiple scattering processes. It is of order $r_{\mathrm{M}} \approx 100\,\mathrm{m}$ for interactions that are relevant here, and in general depends on the density of the considered material [**moliere1947theorie**].
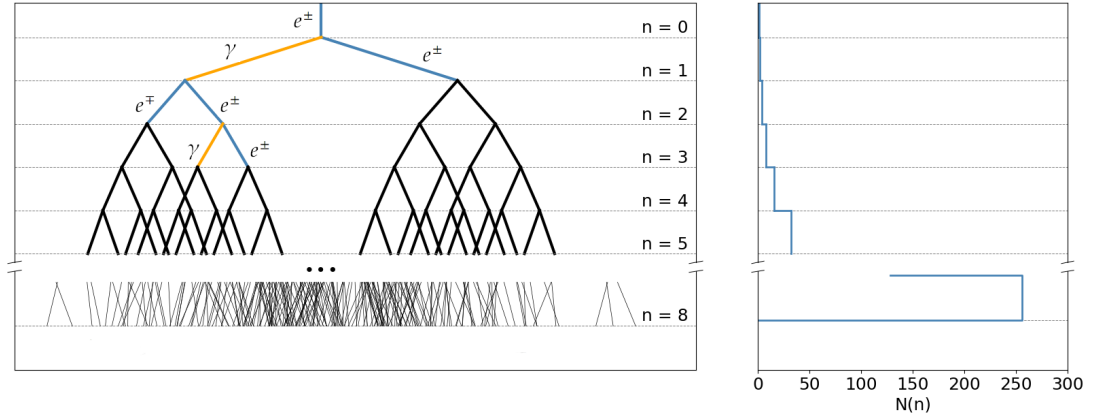
Figure 1.2: Shown on the left is the stylized propagation of an extensive air shower through the atmosphere according to the Heitler-model, quantized in units of X_0. The energy of the primary particle is of order $2^8 \cdot E_c$, which allows for 8 bifurcation steps, and $N_{\max} = 256$ shower particles. The multiplicity of the shower after each step is shown in the right subplot.

1.2 Hadronic showers

Hadronic primaries will readily produce color-charged secondaries, as has been shown many times in particle accelerators. In order to model the development of hadronic showers, the model discussed in **??** thus needs to be adjusted. An example theory has been developed by Matthews in 2005. Following the reasoning in [**matthews2005heitler**], after traversing an atmospheric depth corresponding to the hadronic interaction length, a proton creates on average $N_\pi \approx 15$ pions, of which two thirds are charged, and one third is uncharged. Each newly created (charged) particle then repeats this process, kicking off the shower cascade. The corresponding decay channels of the light π-mesons with the largest **B**ranching **R**atios (BR) are

$$\pi^+ \to \mu^+ + \nu_\mu \qquad (\text{BR} \approx 0.9999,\ \tau = 2.6033 \times 10^{-8}\,\text{s } [\textbf{PDG}]),$$
$$\pi^- \to \mu + \bar{\nu}_\mu \qquad (\text{BR} \approx 0.9999,\ \tau = 2.6033 \times 10^{-8}\,\text{s } [\textbf{PDG}]),$$
$$\pi^0 \to 2\gamma \qquad (\text{BR} \approx 0.9882,\ \tau = 8.5 \times 10^{-17}\,\text{s } [\textbf{PDG}]).$$

With a mean lifetime of just attoseconds, the π^0 decay instantly before being able to continue the cascade process. In this fashion, the uncharged particles initiate a Heitler shower as discussed in **??**, by providing high-energy photons. It follows that every hadronic shower has an electromagnetic component. Moreover, assuming that the inherited energy from the parent particle is roughly uniformly distributed among its' children, one third of the remaining energy in the hadronic component is lost to the electromagnetic component per hadronic interaction length.

Similar to the reasoning in **??**, a primary of given energy initiates a shower of a specific multiplicity $N_{\max}$. This is reached after $n_{\max}$ steps, where the energy per particle

$E_{\mathrm{PP}}(n_{\max})$ is below the critical energy E_c at which the mesons ionize rather than continue the cascade. After this last step, the charged pions eventually decay into muons and neutrinos. The shower characteristics in the scope of the Heitler-Matthews model that describe hadronic showers are thus given by

$$N_{\mathrm{had}}(n) = \left(\frac{2\,N_\pi}{3}\right)^n, \qquad E_{\mathrm{PP}}(n) = \frac{E_0}{N_\pi^n}, \qquad n_{\max} = \left\lfloor \log_N\left(\frac{E_0}{E_{c,\mathrm{had}}}\right)\right\rfloor, \qquad (1.5)$$

wheras the maximum multiplicity (ignoring neutrinos) in the shower is calculated as

$$N_{\max,1} = \underbrace{\frac{3}{2}\left(\frac{2}{3}N_\pi\right)^{n_{\max}}}_{\text{Muon component}} + \underbrace{\sum_{k=1}^{n_{\max}-1} \frac{N(k)}{3}\cdot\left\lfloor\frac{E_{\mathrm{PP}}(k)}{E_{c,\mathrm{EM}}}\right\rfloor}_{\text{EM component}}. \qquad (1.6)$$

The muons stemming from pion decay follow a different LDF than the electromagnetic component. Again following the analysis in [**greisen1960cosmic**], the muonic LDF can be recovered as

$$\rho_\mu(N,t) = 18\left(\frac{N}{10^6\cdot r}\right)^{\frac{3}{4}}\cdot\left(1+\frac{r}{320}\right)^{-\frac{5}{2}}. \qquad (1.7)$$

While the above **??** drops of slower $O(r^{-\frac{3}{2}})$ compared to the electromagnetic component ($O(r^{-3})$), the immediate vicinity of the shower axis contains mostly photons and leptons from the EM subshower. Further out, the muonic component takes over. This is visualized in **??**. Due to this reason, and the fact that muons can carry considerable amounts of energy faraway from the shower axis, the muonic footprint of a shower often appears much more "patchy" compared to the EM portion. This knowledge is espically useful when distinguishing between hadron- and photon-induced air showers (compare [**capistran2015new**]).

1.3 Composite primaries

As is evident from the discussion in **??**, not only single protons (which are strictly speaking also composite) or elementary particles like photons, electrons, etc. appear in the cosmic ray spectrum. Any and all kind of elements can and do appear as possible primaries, given that they are stable to weak decay and can be effectively accelerated near a CR source. The consequence of different primaries on resulting shower characteristics is subtle, but large enough such that it can be used for identification purposes.

Assuming the constituents in a CR nucleus all coherently interact with an air molecule, one arrives at the superposition principle for extensive air showers. It states that for a composite primary with $A = N + Z$ neutrons and protons, each constituent particle will initiate a shower with initial energy of $E'_0 = E_0\,/\,A$, where E_0 is the initial energy
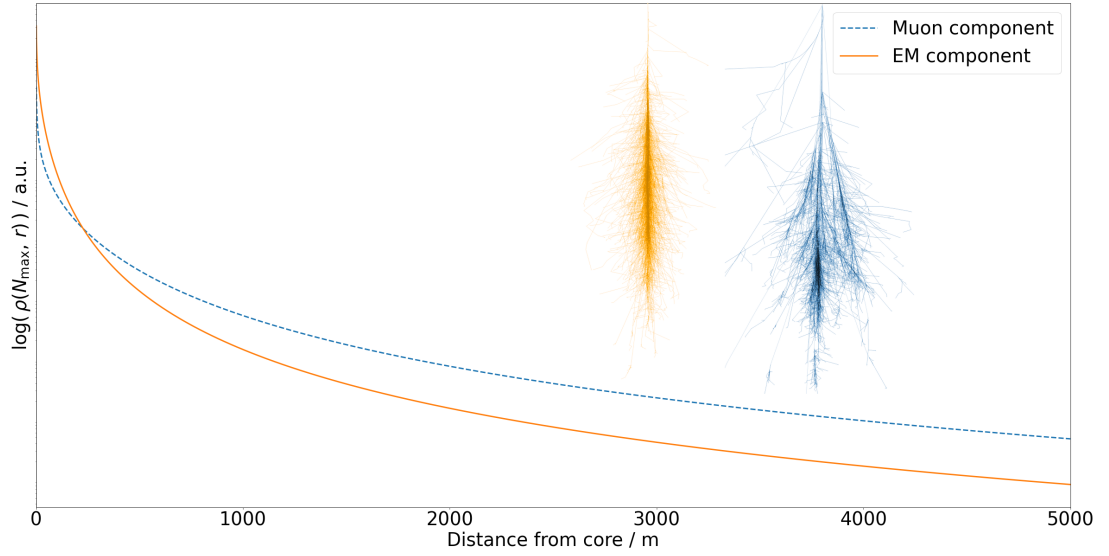
Figure 1.3: The lateral distribution function for the muonic (steelblue) and electromagnetic (orange) component of a vertical, 100 GeV proton shower at roughly sea level ($r_M = 100$ m). The inset plots on the top-right represent the xz-projection of the shower shape. Both images adopted with changes from [**CorsikaShower**].

of the composite particle. It follows that air showers from heaver primaries occur at higher altitudes (lower atmospheric depth X) and with higher particle counts.

$$N_{\max, A} = A \cdot N_{\max, 1}, \qquad n_{\max, A} = \left\lfloor \log_N \left(\frac{E_0}{E_{c, \text{had}}} \right) - \log_N A \right\rfloor, \qquad (1.8)$$

where $N_{\max, 1}$ refers to a proton shower as established in **??**.

1.4 Comments on validity

The Heitler model and Heitler-Matthews model discussed in **??** and **??** respectively make only very rudimentary assumptions on the underlaying physics of particle cascades. Nevertheless, the equations recovered from these assumptions are already a close approximation of real world processes up to $X_{\max}$.

Of course, adding a stochastic component to the above assumptions (c.f. [**MartinShowerSim**]) improves predictions. But even full-fledged Monte-Carlo simulation software frameworks like GEANT4 [**agostinelli2003geant4**] or CORSIKA [**heck1998corsika**] show discrepancies between observed and predicted shower development. An example of this is presented in **??**.

While shower-to-shower fluctuations can explain discrepancies to a degree, there also exist systematic differences between the simulated and observed extensive air showers. These are largely owed to imprecise knowledge of the underlaying physical processes.
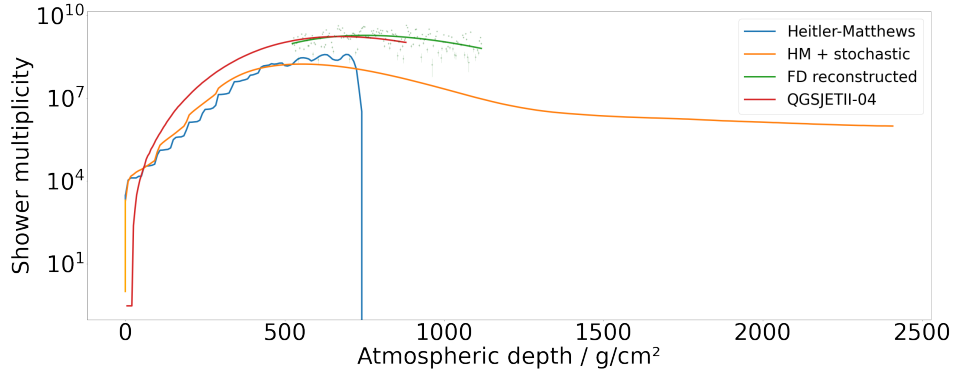
Figure 1.4: Comparison of the number of charged particles for different physics models to reconstructed observations from a 3 EeV proton shower. Shown in steelblue and orange is the Heitler-Matthews model as described in **??**, and extended with a stochastic component. An example of a more in-depth simulation in red, and observed shower multiplicities in green.

For example, hadronic interaction models (e.g. QGSJETII-04 shown in **??**) rely on extrapolation of measured cross sections in the GeV-TeV scales to the relevant CR energies [**ostapchenko2006qgsjet**]. While this is not an unfair assumption given the scale invariance of deep inelastic scattering [**fox1974early**], it is clear, that the approach cannot accurately encompass all effects that may take place at high energies.

In conclusion, the particle cascades evolving from relativistic CRs impinging on earth are still not fully understood. Several simulation frameworks have been developed, which each have their own shortcomings. It is therefore important to compare not only results from simulations using one framework to observations, but also different simulations with each other.

1.5 Detection methods

1.5.1 Cherenkov light

When a charged particle exceeds the phase velocity of light in a medium with refractive index n, the optical equivalent of a sonic boom occurs. Photons travel in a shockwave along an angle $\theta = \arccos\left(n^{-1}\beta^{-1}\right)$ relative to the trajectory of the particle while $\beta \geq \frac{c}{n}$. This process is well understood and can be used to detect high energy cosmic rays.

Imaging Air Cherenkov Telescope

The refractive index of air ranges from 1 in the near vacuum of the upper atmosphere to $\approx 1 + 2.9 \cdot 10^{-4}$ at sea level [**andrews1992analytical**]. This implies that particles with

a Lorentz factor $\gamma \gtrsim 41.5$ emit Cherenkov light, which is satisfied for e.g. muons and protons in the low GeV ranges and above.

It can therefore be expected that extensive air showers, which contain high energy charged particles, produce considerable amounts of Cherenkov light when propagating throught the atmosphere. This light, and by extension the air shower can be detected with **I**maging **A**ir **C**herenkov **T**elescopes (IACTs). Ground based experiments such as VERITAS [**VeritasTelescope**] or H.E.S.S [**HessTelescope**] detect gamma-rays using this technique.

Water Cherenkov Detector

The lightspeed in water is roughly 33% slower than in vacuum. Cherenkov radiation in water therefore occurs more easily than in air. Using this reasoning, a water tank equipped with means of detecting the emitted Cherenkov light, via e.g. **P**hoto**M**ultiplier **T**ubes (PMTs), should be able to measure traces of an air shower.

Indeed, this exact measurement principle of a **W**ater **C**herenkov **D**etector (WCD) was and is adopted in a variety of cosmic ray observatories such as the Pierre Auger observatory [**PierreAugerObservatory**], HAWC [**HAWC**], or Kamiokande [**Kamiokande**], for example.

1.5.2 Fluoresence

Ionization losses have been ignored in the discussion of the formation of extensive air showers. This is of course not completely accurate. During the development of an extensive air showers, particles excite, or even ionize the permeated medium. Consequently, spontaneous emission of photons due to recombination, or transition back to a ground state can be observed. The amount of fluorescence light produced in this way is a gauge for the number of particles present in the shower at a given moment.

In Air

The predominant element in air is nitrogen (78%), whose transitions lay in the UV-band [**FDReconstruction**]. After a nitrogen molecule is excited by a passing shower particle, a photon with wavelength $300\,\mathrm{nm} \leq \lambda \leq 430\,\mathrm{nm}$ is emitted isotropically due to relaxation. The low attenuation of ultraviolet radiation in air allows the fluorescence light to travel large distances before being absorbed [**elterman1968uv**]. This enables cameras like EUSO-TA [**abdellaoui2018euso**] or the **F**lourescence **D**etector (FD) of the Pierre Auger observatory (see [**FDReconstruction**] and **??**) to observe traces of extensive air showers from faraway during their development.

However, because of the low light yield of just $5\,\mathrm{photons/MeV}$ [**nagano2004new**], the detectors must operate in low UV-noise conditions, which places an upper limit on their duty cycle.

In Scintillators

Conventional plastic scintillators have a light yield, that is $1000 - 10000$ times higher than that of air [**holl1988measurement**]. Such scintillators therefore pose an effective way of measuring a shower footprint on the ground. The Pierre Auger **S**urface **D**etector (SD) is equipped with scintillators. Predecessors like KASCADE [**Kascade**] have been using scintillation light to detect cosmic rays as well.

1.5.3 Radio Emission

Relativistic charged particles in the cascade are subject to deflections due to the geomagnetic field. This deflection is largest for $e^{\pm}$ due to their comparably tiny masses. Albeit the deflection of a typical electron in the shower is miniscule and the subsequent emission of Bremsstrahlung tiny, coherence effects along the entire shower front can greatly amplify the electric field strengths obtained from this effect [**schroeder2017radio**]. This gives rise to radio signals emitted by the extensive air shower, which can in principle be detected via antennas.

One challenge in constructing an efficient CR radio detector is the requirement for a radio-quiet environment, where a large enough **S**ignal-to-**N**oise-**R**atio (SNR) permits analysis of measured data. This is the case for the AERA component of the Pierre Auger observatory, which has been in operation since cite. Its results have in part lead the proposal of a vast radio array, GRAND cite, which will have an enormous exposure to CR showers, if built.